

Two-Color System by Red/Cyan Projections Not Land

Hiroaki Kotera; Kotera Imaging Laboratory, Chiba, Japan

Abstract

This paper challenges to a full-color-like reproduction from two primary color separations. In the mid 1950's, Edwin Land accidentally observed a colorful image on the screen projected from two red and green monochromatic separations lit by red and white illuminations. This phenomenon is well known as Land's two-color system, but why the so colorful image appears is not completely solved yet, but has stimulated the basic researches to explore the mystery behind the human color appearance.

The motivation to the 2-color system started from an interest in solving a sort of ill-conditioned color estimation problem, not in the color vision theory. The paper tried to what extent a full-color-like reproduction is possible from a set of two-primary colors as a signal estimation problem. A simplified complementary 2-color system by Red/Cyan projections is newly proposed

Paying an attention to the Red primary as most important, the proposed model demonstrates the excellent performance in a full-color-like reproduction from the Red/Cyan projections different from Red/White Land system. The paper discusses a reduction to 2color-to-2color from 2color-to-3color system. The simplified 2-color model may be applied to any 2-color print system with a cheap set of specified process color inks in the area of quick/convenience or newspaper printing industries.

Introduction

Tracing the revolution of mammals, our common ancestors had USML 4-color sensors in Ultraviolet-, Short-, Middle-, and Long-wavelengths, but degenerated to dichromatic nocturnal vision in the Mesozoic age of the dinosaur. After the extinction of dinosaur, the primate color vision recovered its diurnal trichromacy about 35 million years ago. Through the long-long genetic inheritance process, *L-cones* are duplicated and the halves are mutated to *M-cones* creating a new set of *L-* and *M-cones*. Since the *M-cone* gene has a very similar protein composition to the *L-cone*, the spectral sensitivities of both cones are very close each other. Thus human vision got the present *LMS* trichromacy with the surviving short *S-cone* [1].

In the mid 1950's, Edwin Land accidentally observed a colorful image on the screen projected from two *Red* and *Green* monochromatic separations lit by *Red* and *White* illuminations [2], [3]. This phenomenon is well known as Land's two-color system but why the so colorful image appears is not completely solved yet. This epoch has stimulated the deep interests in the basic researches to explore the mystery behind the human color vision.

At the dawn of color TV age, the exciting Land's model led a development of prototype Red/White TV by Texas Instruments in USA and also Red/Green trial TV product by ORICO color television (1961) in Japan.

The author challenged a full-color estimation problem from 2-color signals scanned with the specified color filters [4], [5]. Afterward, V. C. Cardei reported the similar trial [6].

This paper challenges again to what extent a full-color-like reproduction is possible from a set of two-primary colors as an ill-conditioned estimation problem. Paying an attention to the Red primary color as most important, the proposed model demonstrates an interest result in full-color-like image renditions from Red/Cyan projections different from Red/White Land's system.

The paper discusses a model on the 2color-to-3color and the reduced 2color-to-2color reproductions. The simplified 2-color model may be applicable to a 2-color print system with a cheap set of process color inks in the quick convenience printing industries.

Land's 2-Color System

A Simple Interpretation but incorrect

Land's 2-color system is simply understood as the *Red/White* projections of two monochromatic *Red/Green* color separations as illustrated in **Fig.1**. The *Red* and *Green* separations are overlaid each other on a screen through two projectors with a *Red* filter for *Red* and without filter for *Green* both lit by a white illuminant.

If the *Red* and *Green* projections are mixed on the screen with the ratios of *r* and *g* respectively, the reproduced color \hat{C} is arithmetically described as

$$\hat{C} = \begin{bmatrix} \hat{R} \\ \hat{G} \\ \hat{B} \end{bmatrix} = \begin{bmatrix} rR \\ 0 \\ 0 \end{bmatrix} + \begin{bmatrix} gG \\ gG \\ gG \end{bmatrix} = \begin{bmatrix} rR + gG \\ gG \\ gG \end{bmatrix}. \quad (1)$$

This means the *Green* component is equally shared with *RGB* channels by a *White* projection. However, it'll be obvious that the color *C* must have the excessive *Red* component due to the contribution from *Green* component.

Indeed, a simulated result by Eq. (1) was quite unnatural as shown in **Fig.2 (a)**. Of course, the description by Eq. (1) may be incorrect because the illuminant might not be white and the red filter also might not have an ideal spectral transmittance.

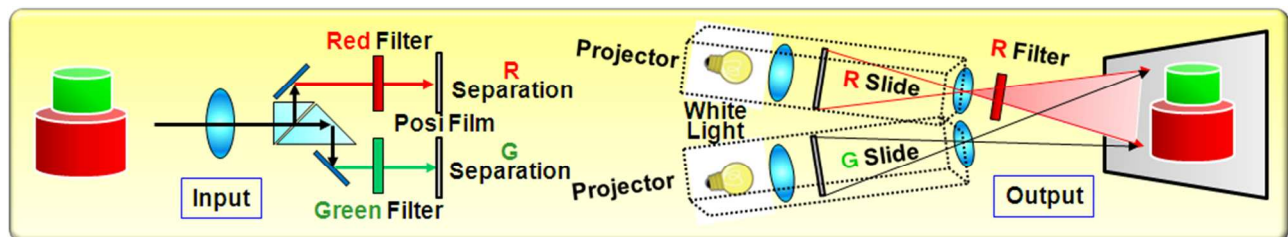


Figure 1 Schematic Illustration of Land's 2-Color System

About 20 years ago, the author had a chance to visit the Rowland Institute at Harvard and fortunately experienced to see the revived Land's 2-color experiments with the same Red/Green color separations used in old days. If the author remembers correctly, the reproduced images by Red/White projections were so colorful and natural, though displayed in the dark room.

Actual Analytical R/W Model by McCann et al

J. McCann et al [4] analyzed the spectral distributions of the Red/White illuminations from the used 3200K tungsten lamp with the combination of Wratten filters and estimated the contributions to XYZ₁₉₆₄ tri-stimulus values from the Red/Green separations.

According to this report, the sRGB image is simulated as

$$\hat{C}_{sRGB} = \begin{bmatrix} \hat{R} \\ \hat{G} \\ \hat{B} \end{bmatrix} \cong [M_{XYZ \Rightarrow sRGB}] \begin{bmatrix} 0.50 & 0.50 \\ 0.34 & 0.66 \\ 0.00 & 1.00 \end{bmatrix} \begin{bmatrix} R \\ G \end{bmatrix}. \quad (2)$$

The simulated image by Eq. (2) is shown in Fig.2 (c). It's very colorful and much better than Fig.2 (b), but looks to be still unsatisfactory in the reproduction of Reddish petals of carnation.



(a) Original (b) Simple Land model (c) Analytical McCann

Figure 2. Sample by Red/White 2-col projections system

The original R/W Land's system is based on a concept of 2color-to-2color reproduction, that is, both inputs and outputs are limited to two-primaries. This concept has a great advantage in practice, because if realized, very simple-structured and/or very low-cost display/print devices could be designed, even if not true-color but full-color-like.

This paper also challenges to a 2color-to-2color system through the following two-steps:

[Step1] 2color-to-3color estimation

A lost color channel in RGB is recovered from the remaining two channels by the signal estimation methods

[Step2] 2color-to-2color simplification

The estimated RGB in step1 is reduced to 2color expression.

2Color-to-3Color Estimation

As an inverse problem from low-to-high dimensions, here, the tri-color reproduction is tried by the spectral estimation methods from the reduced 2-color signals.

As the candidates for inverse estimation,

[A] Pseudo-inverse estimator

[B] Smoothed-inverse estimator

[C] Wiener-inverse estimator

are tested for the simulations. Through the experiments with typical natural color images, the performances are ranked in the order of [C], [B], and [A].

Of course the color appearances depend on the image contents. Though the method [B] occasionally brought the better results than [C], Wiener estimator worked best in most cases.

Fig.3 overviews the spectral estimation model from 2-colors.

Now assuming 2-color sensors with the spectral sensitivity function S consisting of any color matching function (cmf), the 2-color vector signal Q is described by

$$\begin{aligned} Q &= [PQ]^t = S^t \rho + e, \quad e = \text{noise} \\ \text{where, } S &= [\bar{p}(\lambda) \bar{q}(\lambda)] = \text{sensor spectral sensitivities.} \\ \rho &= [\rho_{\lambda 1} \rho_{\lambda 2} \dots \rho_{\lambda n}]^t = \text{input spectral reflectance} \end{aligned} \quad (3)$$

Where, the sensor's spectral sensitivity function $[\bar{p}(\lambda) \bar{q}(\lambda)]$ is selected as a 2-color combination of CIE1931 $\bar{x}(\lambda) \bar{y}(\lambda) \bar{z}(\lambda)$ or sRGB $\bar{r}(\lambda) \bar{g}(\lambda) \bar{b}(\lambda)$ or LMS $l(\lambda) m(\lambda) s(\lambda)$ cmfs.

Operating an inverse estimator Φ_{inv} on the vector Q , the spectral reflectance is estimated as $\hat{\rho}$ and displayed as the sRGB image, for example, like as

$$\begin{aligned} \hat{\rho} &\cong \Phi_{inv} Q \\ sRGB_{img} &= (M_{XYZ \Rightarrow sRGB}) A^t \hat{\rho} \\ \text{where, } A &= [\bar{x}(\lambda) \bar{y}(\lambda) \bar{z}(\lambda)]: \text{xyz cmf} \end{aligned} \quad (4)$$

The following sections refer to the smoothed inverse estimator $\Phi_{inv} = S_{SMT}$ and the Wiener inverse estimator $\Phi_{inv} = W_{inv}$.

Smoothed Inverse Estimator

Since the color objects in nature have the gentle and smoothed spectral shapes, minimum-norm estimation with the constrained smoothness provides the better solution.

Taking the second derivative of spectral input ρ by applying the Laplacian operator D , the edge vector δ is obtained as

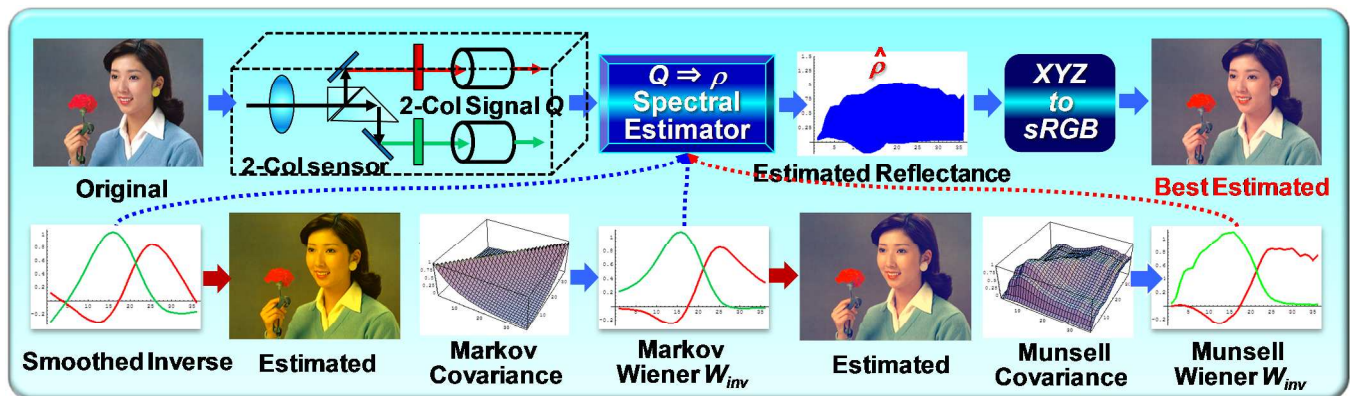


Figure 3 Schematic Illustration of 2Color-to-3Color Spectral Estimation Model

$$\delta = \begin{bmatrix} \delta_1 \\ \delta_2 \\ \vdots \\ \delta_{n-2} \end{bmatrix} = \begin{bmatrix} 1-2 & 1 & 0 & 0 \cdots 0 \\ 0 & 1-2 & 1 & 0 \cdots 0 \\ \vdots & \vdots & \vdots & \vdots \\ 0 & \cdots \cdots 0 & 1-2 & 1 \end{bmatrix} \begin{bmatrix} \rho_1 \\ \rho_2 \\ \vdots \\ \rho_n \end{bmatrix} = \mathbf{D}\rho. \quad (5)$$

Because δ reflects “edge” component, its quadratic norm will be a smoothness measure as

$$\delta^t \delta = \sum_{i=1}^{n-2} \delta_i^2 = \rho^t \mathbf{D}^t \mathbf{D} \rho = \rho^t \mathbf{N} \rho = \|\rho\|_N^2. \quad (6)$$

$$\mathbf{N} = \mathbf{D}^t \mathbf{D} = \begin{bmatrix} 1 & -2 & 1 & 0 & \cdots \cdots \cdots 0 \\ -2 & 5 & -4 & 1 & 0 & \cdots \cdots \cdots 0 \\ 1 & -4 & 6 & -4 & 1 & 0 & \cdots \cdots \cdots 0 \\ 0 & 1 & -4 & 6 & -4 & 1 & 0 \cdots \cdots 0 \\ \vdots & \vdots & \vdots & \vdots & \vdots & \vdots & \vdots \\ 0 & \cdots \cdots \cdots 0 & 1 & -4 & 6 & -4 & 1 \end{bmatrix}. \quad (7)$$

Now introducing *Lagrange* multiplier λ to minimize Eq. (6) under the smoothing matrix \mathbf{N} ,

$$J(\rho) = \rho^t \mathbf{N} \rho + \lambda^t (\mathbf{S}^t \rho - \mathbf{Q}), \quad (8)$$

The scalar term $J(\rho)$ is minimized when its first derivative is zero

$$\partial J(\rho) / \partial \rho = 2\mathbf{N}\rho + \lambda \mathbf{S} = 0, \quad (9)$$

Solving Eq. (9) under Eq. (4), we get the solution as

$$\hat{\rho} \cong \mathbf{S}_{SMT}^{-1} \mathbf{Q}, \quad \mathbf{S}_{SMT} = \mathbf{N}^{-1} \mathbf{S} (\mathbf{S}^t \mathbf{N}^{-1} \mathbf{S})^{-1} \quad (10)$$

for $\mathbf{N} = \mathbf{N} + \varepsilon \mathbf{I} \ (\varepsilon \ll 1)$

Here, since matrix \mathbf{N} is singular, a small perturbation ε is added to be non-singular [7].

Wiener Inverse Estimator

Wiener-inverse is a popular estimator to minimize the *MSE*

$$e^2 = E[(\rho - \hat{\rho})^t (\rho - \hat{\rho})]. \quad (11)$$

The solution is given by

$$\hat{\rho} \cong \mathbf{W}_{inv} \mathbf{Q} + \mathbf{b}$$

where, $\mathbf{W}_{inv} = \mathbf{R}_{CC} \mathbf{S} (\mathbf{S}^t \mathbf{R}_{\rho\rho} \mathbf{S} + \mathbf{R}_{ee})^{-1}$

$$\mathbf{R}_{\rho\rho} = \text{covariance matrix}, \mathbf{R}_{ee} = \text{noise variance} \quad (12)$$

$\mathbf{b} = \mathbf{m}_C - \mathbf{W}_{inv} \mathbf{S}^t \mathbf{m}_C$: bias, $\mathbf{m}_C = \text{mean vector}$

The bias term \mathbf{b} is usually ignored as small, but here $m_C \cong 0.3$ is used as a default value for general case [7].

Though the true covariance matrix $\mathbf{R}_{\rho\rho}$ is obtained from any trained samples, the Markov model is often used for non-parametric Wiener estimation. Assuming a strong correlation with coefficient τ between the adjacent spectral components, the Markov covariance matrix $\mathbf{R}_{\rho\rho}$ is modeled by

$$\Sigma_{\rho\rho} = \begin{bmatrix} 1 & \tau & \tau^2 & \cdots \cdots \cdots \tau^{n-1} \\ \tau & 1 & \tau & \tau^2 & \cdots \cdots \tau^{n-2} \\ \tau^2 & \tau & 1 & \tau & \cdots \cdots \vdots \\ \vdots & \vdots & \vdots & \vdots & \ddots \\ \tau^{n-1} & \tau^{n-2} & \cdots \cdots \cdots 1 \end{bmatrix}. \quad (13)$$

In the simulation experiments, the covariance matrix $\mathbf{R}_{\rho\rho}$ trained from the spectral Munsell chips (1600 colors) gave the better performance than Markov covariance matrix in most cases.

Fig.4 shows the typical simulation results in the Wiener-inverse and the Smoothed-inverse estimations. As a quality common to all, the renditions from the 2-primaries of *RG/XY/LM* are nice in color, while those from *GB/YZ/MS* give unnatural appearance. This means the long-wavelength primary must be most important and that of short-wavelength may be least important. In addition, the average color differences don't always reflect the subjective appearance.

Simplified 2Color-to-2Color System

The 2col-to-3color estimation model resulted in considerably good color renditions in spite of the inverse projection from only 2-dimensional signals to the higher dimensional spectra ($n=36$, $\lambda=380\sim 730$ nm, $\Delta\lambda=10$ nm). However, it needs 3 primary colors to reproduce the estimated images on the output display or color printer.

If the reproduced tri-color images could be represented by only 2-primary colors just as same as the original Land's 2-color system, an innovative application will be expected. Even if not true-color, a full-color-like imaging may be useful for a simple-structured easy 2-color electronic paper or an economical quick/convenience printing or newspaper publishing without using expensive color inks.

Through the experiments, the unsupervised Wiener estimator with the covariance matrix trained by spectral Munsell chips worked in stable for the typical test images. Here, the simplification of Wiener estimator to a 2color-to-2color system is examined as follows.

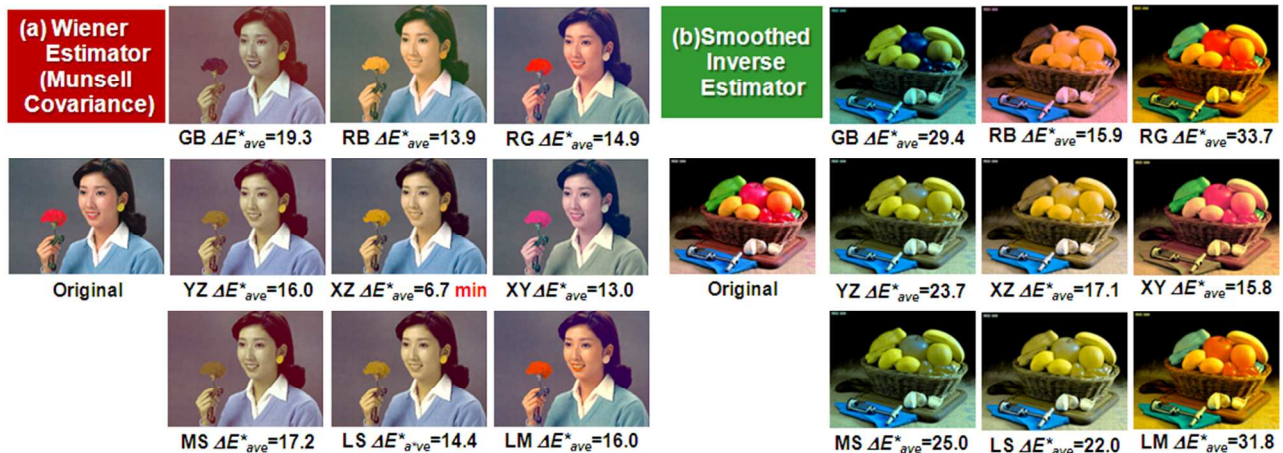


Figure 4 Schematic Illustration of 2Color-to-3Color Spectral Estimation Model

Compact Transform Equation

The reproduced *sRGB* images from estimated spectral reflectance in Eq. (4) is simply rewritten as

$$\begin{aligned} sRGB_{img} &= (M_{XYZ \rightarrow sRGB}) A' \hat{\rho} \\ &= (M_{XYZ \rightarrow sRGB}) \hat{\Phi}_{inv} Q = M_{3 \times 2} Q \end{aligned} \quad (14)$$

Letting the 2-color signal be $Q = [R \ G]^t$, Eq. (14) is described as

$$sRGB_{img} = \begin{bmatrix} \hat{R}_{img} \\ \hat{G}_{img} \\ \hat{B}_{img} \end{bmatrix} \cong M_{3 \times 2} Q = \begin{bmatrix} r_R & r_G \\ g_R & g_G \\ b_R & b_G \end{bmatrix} \begin{bmatrix} R \\ G \end{bmatrix}. \quad (15)$$

In case of Wiener estimator, the 3x2 matrix $M_{3 \times 2}$ is given as

$$\begin{aligned} M_{3 \times 2} &= (M_{XYZ \rightarrow sRGB}) A' W_{inv} \\ &= (M_{XYZ \rightarrow sRGB}) A' \Sigma_{pp} S (S' \Sigma_{pp} S + \Sigma_{ee})^{-1}. \end{aligned} \quad (16)$$

Using the covariance matrix obtained from Munsell spectral color chips (1600 colors) and neglecting the noise, $M_{3 \times 2}$ is calculated in the case of $Q = [R \ G]^t$ for $S = [\bar{r}(\lambda) \ \bar{g}(\lambda)]$ as a constant value of

$$M_{3 \times 2} = \begin{bmatrix} 1.206 & 0.0 \\ 0.0 & 0.948 \\ -0.142 & 0.694 \end{bmatrix}. \quad (17)$$

Although the tri-color image is reproduced from the 2-color signal Q in each pixel, it is notable that the transform matrix $M_{3 \times 2}$ is an image-independent constant.

A New 2-Color System by Red/Cyan Projections

Red/Cyan 2color Projection System

The descriptions in Eq. (14) ~ Eq. (16) are originated from the complex spectral Wiener estimation, but finally condensed to a simple linear transformation with matrix $M_{3 \times 2}$. However, since this compact Eq. (15) denotes a 2color-to-3color system, it still needs 3-primary colors in the output stage.

A one of easy ways to reduce Eq. (15) into a 2col-to-2col system is to round the coefficients in the matrix $M_{3 \times 2}$.

For example, suppressing the coefficient for the *Red* signal not to exceed than 1.0 and rounding the coefficients roughly to the following like as

$$M_{3 \times 2} = \begin{bmatrix} 1.0 & 0.0 \\ 0.0 & 1.0 \\ 0.0 & 0.7 \end{bmatrix}, \quad (18)$$

Eq. (15) is further simplified into 2col-to-2col system as

$$\begin{aligned} sRGB_{img} &= \begin{bmatrix} \hat{R}_{img} \\ \hat{G}_{img} \\ \hat{B}_{img} \end{bmatrix} \cong \begin{bmatrix} 1.0 & 0.0 \\ 0.0 & 1.0 \\ 0.0 & 0.7 \end{bmatrix} \begin{bmatrix} R \\ G \end{bmatrix} = \begin{bmatrix} 1.0 \\ 0.0 \\ 0.0 \end{bmatrix} R + \begin{bmatrix} 0.0 \\ 1.0 \\ 0.7 \end{bmatrix} G \\ &= k_R R + k_C G \end{aligned} \quad (19)$$

Eq. (19) means the *sRGB* image is reproduced by the mixture of specified two primary colors of *Red/Cyan*. The first vector k_R is a simple gain factor, while the second vector k_C denotes a *Cyan-like* filter. That is to say, a full-color-like reproduction is possible by a mixture of *Red* and *Cyan-filtered Green* components.

Fig.5 shows a reproduced sample by Eq. (19) derived from the Wiener estimator W_{inv} using the Munsell covariance matrix Σ_{pp} .

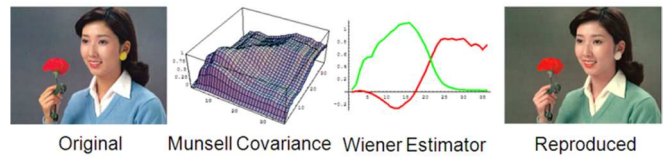


Figure 5. Sample rounded to Red/Cyan 2-color system from Wiener model

Because the red gain factor k_R had better to be rounded to a unit vector u , a generalized *Red/Cyan* projections is modeled again by

$$\begin{aligned} sRGB_{img} &= \begin{bmatrix} \hat{R}_{img} \\ \hat{G}_{img} \\ \hat{B}_{img} \end{bmatrix} \cong uR + k_C G \\ \text{where, } u &= \begin{bmatrix} 1.0 \\ 0.0 \\ 0.0 \end{bmatrix} : \text{unit vector, } k_C = \begin{bmatrix} 0.0 \\ g_G \\ b_G \end{bmatrix} : \text{Cyan filter} \end{aligned} \quad (20)$$

In summary, the proposed simple 2-color system by *Red/Cyan* projections is schematically illustrated in **Fig.6**. The proposed system is fundamentally different from the original Land's system on that point of using *Cyan* as a substitute for *White*.

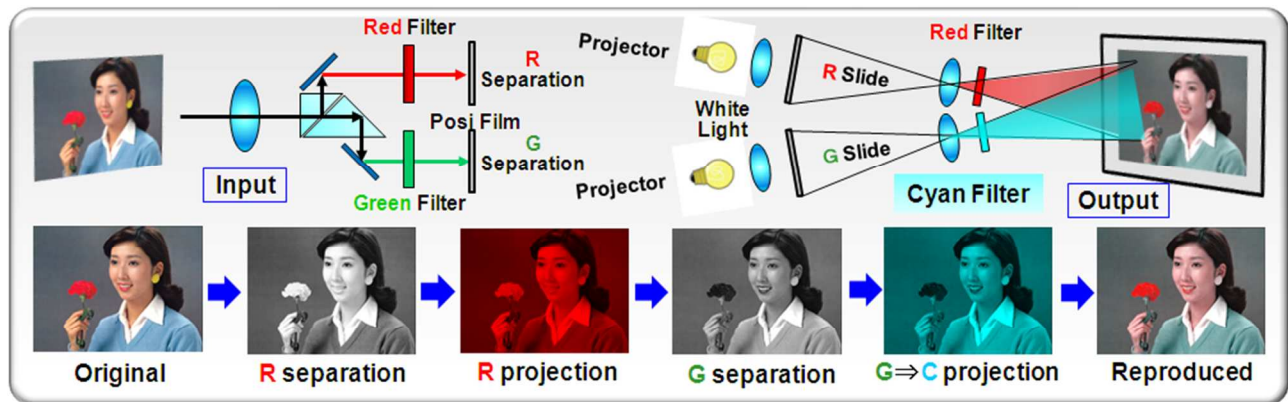


Figure 6. Schematic Illustration of Proposed Red/Cyan 2-Color Projection System

Red/Cyan Complement 2-Color system

The matrix $M_{3 \times 2}$ depends on the estimation models and is not almighty for every image, of course. But, it was surprising the vector $k_C \approx [0 \ 1 \ 1]^T$ close to a pure Cyan succeeded in unexpectedly nice full-color-like reproductions in many cases.

The case of pure Red/Cyan projections is simply understood as the Red separation is projected as it is, while the Green separation is projected passing through the pure Cyan filter. This model may be

called as Red/Cyan complement 2-color system, where Red-Green is an opponent-color and Red/Cyan is a complement-color pairs.

In general, the Red/Cyan complement 2-color system is regarded as a special case in the Red/Cyan 2color projection system derived from the simplified Wiener estimator.

Fig.7 shows some samples by the Red/Cyan complementary 2-color system in comparison with the analytical Land model by McCann.

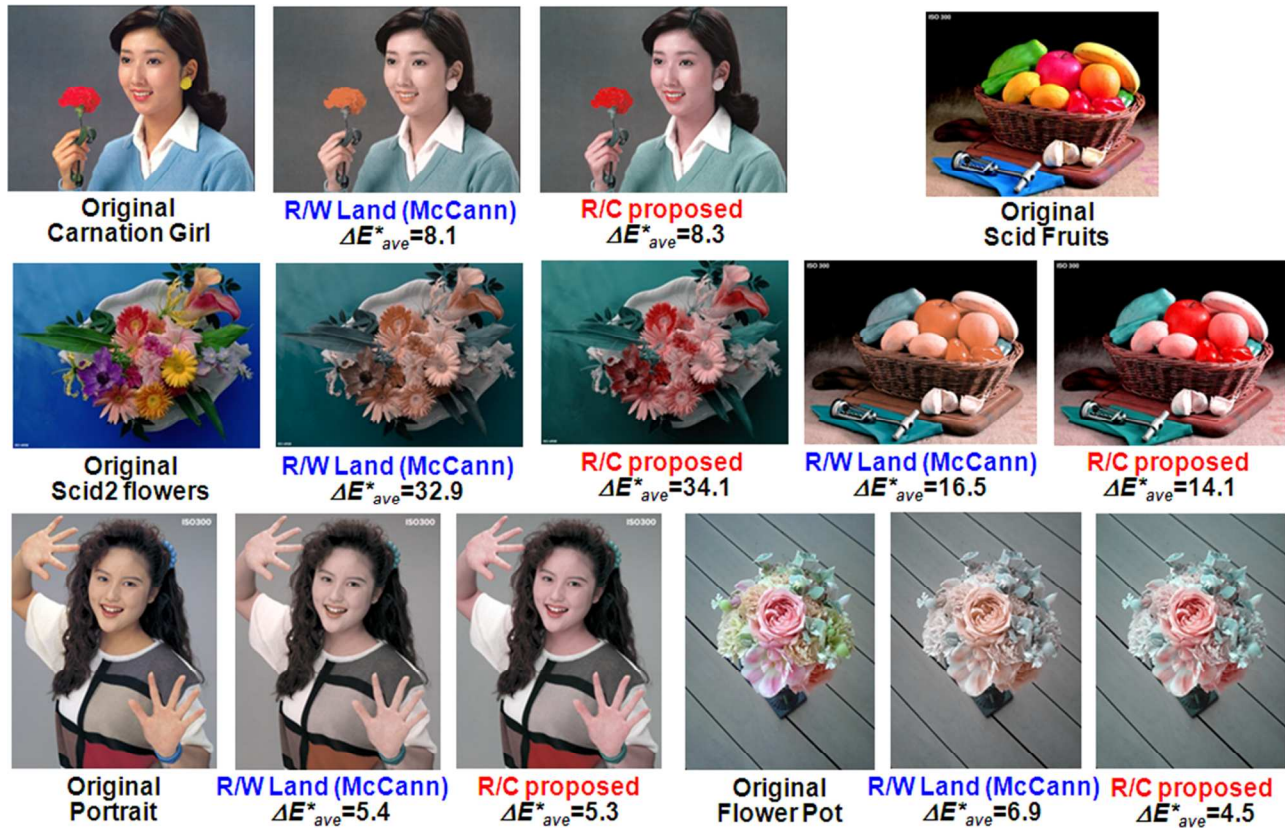


Figure 7. Samples by proposed Red/Cyan complement 2-color system in comparison with analytical Red/White Land's system

Discussion

Problem in Red/Cyan 2-Color Projection system

In spite of a very rough approximation, the Red/Cyan complementary 2-color system worked very well for the test images such as “carnation girl”, “portrait”, and “flower pot” as shown in Fig.7. The analytical Land model by McCann also worked nice in color reproduction with the color differences ΔE^*_{ab} (mean) less than 10. In detail, the proposed Red/Cyan complementary system resulted in the better renditions for reddish colors than McCann. On the other hand, the SCID test images such as “flowers” or “fruits” may be unacceptable because of large color differences. Though these samples look to be natural at a glance, but the large color differences mainly come from the errors in the large areas of background.

A typical weakness in the Red/Cyan complementary 2-color system appears in the reproduction for “yellowish” colors as shown in Fig.8 (b). Since the “yellow petal” includes less “Blue” but much “Green” components, the petal color goes to “whitish” due to the Cyan filtering to the monochromatic Green component. In contrast to

Fig.8 (b), the “yellow petal” is well reproduced in (c) by the 2color-to-3color smoothed-inverse estimation method. If the use of 3 colors in the output stage is permitted, this problem is solved, but the merit of 2-color display or 2-color printing must be lost.

However, if the coefficient b_G in the vector k_C of Cyan filter in Eq. (20) is changed to the smaller value depending on the image, the reproducibility of “yellow petal” could be improved.

Fig.8 (d) shows an improved result with the coefficient $b_G=0.294$ calculated from the average ratio of RGB pixels in the original image. In order to print this image (d) by 2-color, the process color ink set of Red and the specified Cyan blended to about $k_C=[0.0 \ 1.0 \ 0.3]^T$ is necessary. If the set of 2-color process inks is selectable for inkjet printer depending on the image, an economical short-run printing may be possible.

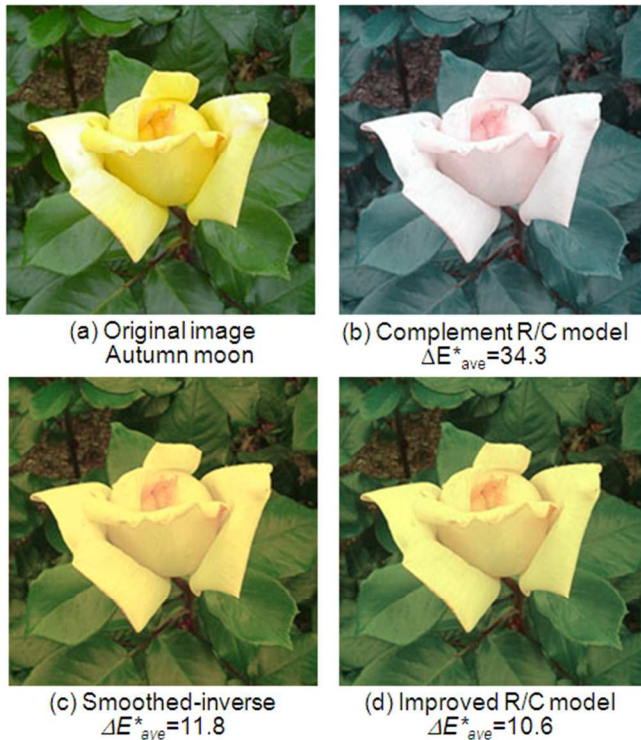


Figure 8. Weakness in Complement Red/Cyan model and Improvement

Color Gamut in 2Col-to-3Col vs. 2Col-to-2Col System

The constraint on the usable primary colors limited to two in the output stage basically reduces the color gamut to 2-dimension. Fig.9 shows a comparison of color gamut between the 2color-to-2color complement Red/Cyan system and 2color-to-3color Wiener estimation model for the test color chips. As clearly seen, the gamut of 2color-to-2color system is compressed to narrower 2-D space, while that of 2color-to-3color system is expanded to 3-D by the interpolation function of estimator.

Although this gamut limitation is theoretically unavoidable, the proposed Red/Cyan projections 2-color system still has an appeal for any possible industrial application such as convenience 2-color printing, low-cost electronic paper, or mobile phone display.

Conclusions

The paper discussed a problem going against the stream of multi-primary-color age. Though the Land's 2-color system might be thought as a relic from the previous century, it still leaves the ceaseless interests in the mystery behind the human color vision.

The proposed 2-color approach started from a standpoint of color signal processing to solve a sort of ill-conditioned estimation problem, not from the color vision theory. The mathematical procedure might be rough rather than rigorous, but found out the Red/Cyan complement 2-color system as an extremely simplified solution. The proposed model, of course, doesn't against the three primary color theory but tells us not true color but a full-color-like reproduction is often permissible unless we see the true original and the imitation side by side.

The analytical Red/White projections model by McCann provided so many hints towards the Red/Cyan complement 2-color model. In practice, for example, a set of specified process color inks and 2-color matching algorithm based on CMS are necessary.

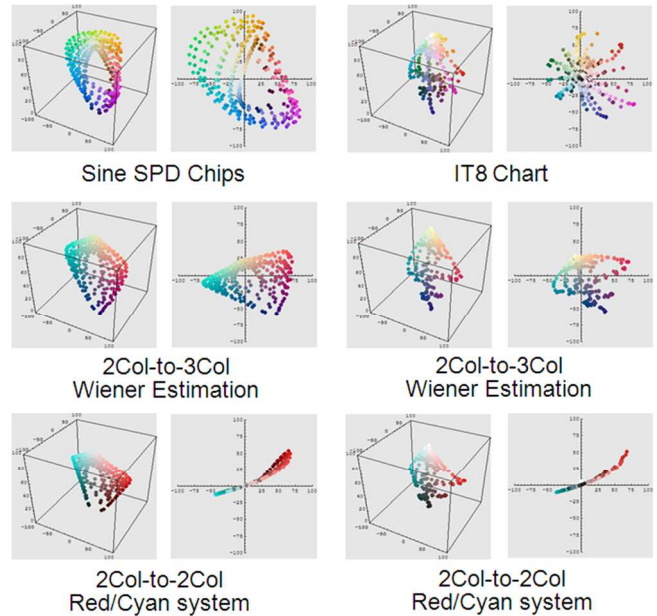


Figure 9. Comparisons in Color Gamut

In addition, the paper is short of more deep study in relation to the latest vision research [9] and lacks in the psycho-physical or color appearance estimation experiments. The furthermore studies on the fundamental two-color vision are left behind as the future works.

References

- [1] Jacobs and Nathans: The Evolution of Primate Color Vision, Scientific American, April 2009-4, 44-51 (2009)
- [2] E. H. Land: Color Vision and the Natural Image Part I & II, Proc. Nat. Acad. Sci., 45, 1, 115-129 ibid, 636-644 (1959)
- [3] M. McCann, editor: Edwin H. Land's Essays, Vol. III, Color Vision, Society IS&T (1993)
- [4] J. McCann et al: Red/White Projections and Rod-Lcone Color: An Annotated Bibliography, J. E. I., 13(01), 8-14 (2004)
- [5] H. Kotera and K. Kanamori: Color Image Rendition from Two Primary Colors: Proc. NIP7 (1991)
- [6] H. Kotera and K. Kanamori: Color Image Rendition from Two Color Separation Signals, JIST, 36, 6, 551-557 (1994)
- [7] C. E. Mancill: Digital Color Image Restoration, USCIP Report, No.630, ARPA Order No. 1706 (1975)
- [8] V. C. Cardei: From Dichromatic to Trichromatic Images; Implications for Image Recovery and Visualization, Proc. IS&T PICS1999
- [9] S. K. Shevell: The Verriest Lecture: Color lessons from space, time and motion, JOSA A, 29, 2, A337-A345 (2012)

Author Biography

Hiroaki Kotera joined Panasonic Corp., in 1963. He received Doctorate from Univ. of Tokyo. After worked at Matsushita Res. Inst. Tokyo during 1973-1996, he was a professor at Dept. Information and Image Sciences, Chiba University until his retirement in 2006. He received 1993 IS&T journal award, 1995 SID Johann Gutenberg prize, 2005 IEEE Chester Sall award, 2006 ISJ journal award, 2007 IS&T Raymond. C. Bowman award, 2009 SPSTJ and 2012 IEEEJ best paper awards. He is a Fellow of IS&T.